Optical Pumping of Rubidium Vapor

D.C. Elton[1, a)] and J. Chia-Yi[b)]
Stony Brook University

(Dated: 27 April 2012)

We studied the hyperfine levels of Rubidium using the technique of optical pumping. Using the equation $\nu_0 = \frac{g_J \mu_0}{h(2I+1)} B$ for Rb-87 we found $g_F = 0.5177 \pm .0002$ and $B_{earth} = 0.416 \pm .0002$. For Rb-85 we found $g_F = 0.342 \pm .0001$ and $B_{earth} = 0.421 \pm .002$. We also looked for evidence of power broadening and compared our lineshapes to Guassian, Lorentzian and Voigt profiles.

The technique of optical pumping which we used was discovered in a series of work by Alfred Kastler in the 1940s, for which he would win the entire Nobel Prize in Physics in 1966. Optical pumping allows one to overcome several difficulties associated with measuring transitions between hyperfine levels in a magnetic field. The first difficulty is that in thermal equilibrium the populations of electrons in two adjacent hyperfine levels are nearly identical. One can calculate the fractional difference between levels using the Boltzmann formula. Assuming a splitting of 1Mhz at room temperature:

$$\frac{n_b}{n_a} = \exp\left(-\frac{E_b - E_a}{kT}\right) = 1 - 2 \times 10^{-7} \tag{1}$$

Thus, it is impossible to measure absorption between these levels, because the processes of emmission and absorption would cancel each other out. Another problem is that the intrinsic decay lifetime for transitions between adjacent states is extremely long – on the order of millions of years. Finally, even if such photons were emitted, they would have frequencies on the order of a few MHz, for which no efficient quantum detector exists.

Optical pumping overcomes these limitations by "pumping" electrons into the highest Zeeman sublevel. To understand how it works, one should be familiar with the origin of the Zeeman levels, a description of which is included in Appendix 1. The important formula is the one for the splitting between Zeeman levels in a weak field:

$$\nu_0 = \frac{g_J \mu_0}{h(2I+1)} B \tag{2}$$

The first-order transitions between adjacent Zeeman levels are magnetic dipole transitions, for which the selection rules are

$$\Delta l = \pm 1 \qquad \Delta j = \pm 1 \qquad \Delta m = \{-1, 0, 1\} \tag{3}$$

In particular, right-handed circularily polarized light will induce $\Delta m = +1$ transitions and left-handed circularily polarized light will induce $\Delta m = +1$ transitions. If one only uses right-handed light, (and sends this light in parallel to the applied magnetic field) then all of the electrons will be pumped to the highest m_F state. Then downward transitions between levels can be induced with an RF field and subsequent absorption of the pumping signal can be observed.

I. EXPERIMENTAL TECHNIQUE

Figure 0 (lost) shows an schematic layout of our apparatus and the equipment that we used. A rubidium lamp provides the pumping light, which is sent through a linear polarizer, a 1/4-wave plate and a filter to isolate the D1 line. This light passes through the Rb sample cell and the transmitted light is detected by a photodiode. A set of Maxwell coils provides the applied B field while a set of Helmholtz coils are used to induce the magnetic resonance transitions.

II. CALCULATION OF B_{earth} AND g_F

The Maxwell coil configuration consists of three coaxial coils: a large central coil "A" with two smaller adjacent coils B and C. Assuming the coils are infinitely thin, the magnetic field due to the Maxwell coil on its axis is:

$$\frac{|B_{coil}|}{I} = \left(\frac{\mu_0 N_B}{2R_B} + \frac{\mu_0 N_{A,C} R_{A,C}^2}{(x^2 + R_{A,C}^2)^{3/2}}\right) = .000421[\mathrm{T/A}] \tag{4}$$

with an error

$$\Delta B_{coil} = \sqrt{5.6 \times 10^{-43} I^2 + 4.43 \times 10^{-16}} \tag{5}$$

For instance, for a current of $1A$ the error in calculating B_{coil} turns out to be .00021 gauss. A more precise calculation takes into account the non-zero thickness of the wires, resulting in the formula

$$|B_{coil}| = .000402I \tag{6}$$

Using the weak field equation we can relate the magnetic field of the coil to the splitting's resonance frequency:

$$B_{coil} = \frac{hf}{\mu_B g_F} - B_{earth} \tag{7}$$

[a)] Electronic mail: daniel.elton@stonybrook.edu
[b)] Electronic mail: thefairfeather@msn.com

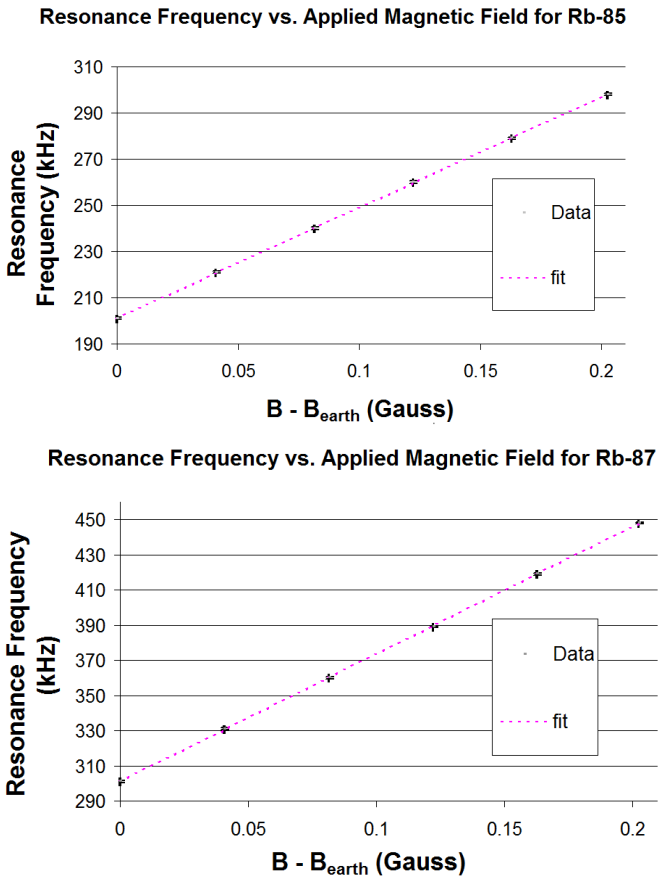

FIG. 1. Resonance frequency vs. magnetic field for Rb-85 and Rb-87

This expression was fit to data we took at currents between 0 and 50 mA (see Figure II). For Rb-87 we found $g_F = 0.5177 \pm .0002$ and $B_{earth} = 0.416 \pm .0002$, with a χ^2/DOF of 6.65. For Rb-85 we found $g_F = 0.342 \pm .0001$ and $B_{earth} = 0.421 \pm .002$ with a χ^2/DOF of 8.05. Neither of these fits were good, with chance probabilites of $p < .15$ and $p < .075$ respectively. These poor fits are probably due to the relatively small number of data points (6) that we used. More data should have been taken in the low-field regime. When data from higher currents (250mA - 2000mA) was included, the quality of the fit decreased. The accepted values for g_F for $J = 1/2, L = 0$ are .3340 for Rb-85 and .50174 for Rb-87. Neither of our measurements lie within our error bars suggesting a source of systematic error in the experiment. In particular, it was noticed that the calculation is very sensitive to the magnetic field to current relationship – hence the importance taking into account the finite volume of the wires. Things we did not take into account were the finite size of the Rb-vapor cell or the magnetic fields due to the lead in wires.

According to the NOAA website, the average magnitude of the Earth's magnetic field at our lattitude and longitude is .523 G. However, it is likely that the field was shielded by the building and/or distorted by local objects in the room, so we consider the field we measured (average $B_{earth} = .419 \pm .001$) to be reasonable.

III. OBSERVATIONS AT HIGHER FIELDS

Figure III shows some of the absorption lines we observed at higher magnetic fields. Unfortunately, only the highest-m lines are most visable, since the rf-induced downward transitions are counteracted by the pumping light. Lowering the pumping light intensity could have solved that problem, at the cost of smaller amplitude peaks. In Rb-87 we noticed small peaks which are due to multiphonon transitions (see the two subfigures in the top right of Figure III). During a 2-photon absorption process, an electron can change it's angular momentum state by $l = +2, 0, \text{or} -2$. The 2-phtonon absoprtion lines are shifted because of the non-linear spacing between the m_F levels.

IV. LINESHAPE BROADENING

There are many factors which contribute to the shape and width of a spectral line. Here we were intrested in the power broadening effect, which can be derived within the context of a two state quantum system. Ignoring other effects apart from the intrinsic "lifetime broadening" and power broadening one finds that the shape of an absorption line is given by (Milloni 217):

$$\frac{N_2(t=\infty)}{N} = \frac{\chi^2\beta/2A_{21}}{\Delta^2 + \beta^2 + \chi^2\beta^2/A_{21}} \tag{8}$$

where χ is the Rabi frequency and $\Delta = \omega_{21} - \omega$. Since χ is proportional to $|E|$, χ^2 is proportional to the intensity of the light.

Unfortunately, in our setup there was also significant pressure broadening. Our Rubidium vapor cell also contains Argon at 50 torr (.07 atm / 6700 Pa), which is used as a buffer gas to prevent collisions between the Rb and the walls of the container. The rate of coillisions in a ideal gas with $P = 50$ torr and $T = 42\,^{\circ}\text{C}$ is (Milonni p96)

$$\beta = \frac{1}{\tau} = 2.69 \times 10^8 \frac{P(\text{Torr})}{T} = 414\text{MHz} \tag{9}$$

This rate is very high – much higher than the typical absorption frequencies, yet such collisions will chiefly effect electric dipole transitions, and not the magnetic dipole transitions we looked at. We did not attempt an analysis of the effect of collisions on magnetic dipole transitions, but based on this high rate of collisions, it seems likely collision broadening may play some role.

There is also Doppler broadening, which results in a Gaussian lineshape. The FWHM of this lineshape (at

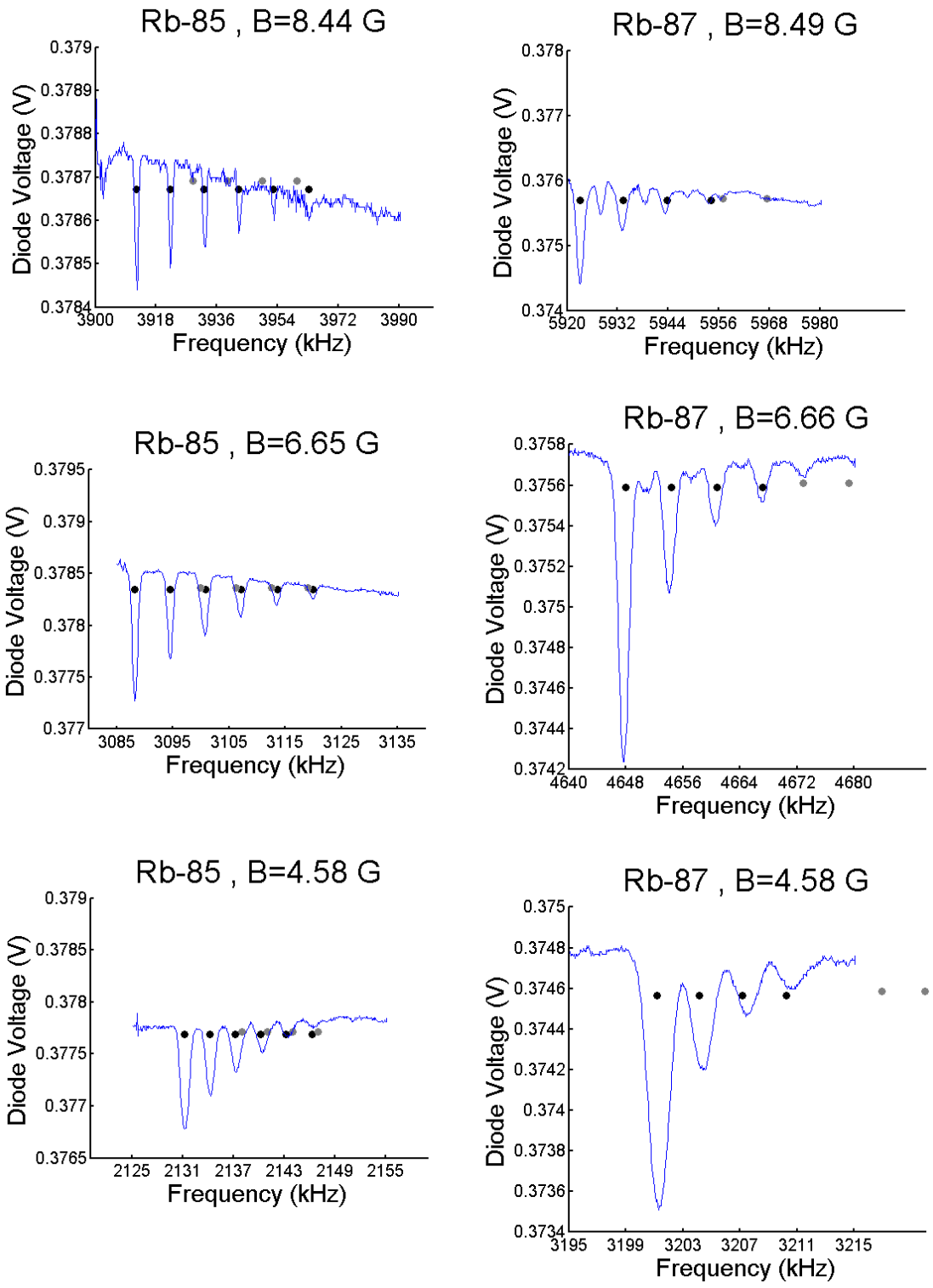

FIG. 2. Absorption lines at a variety of magnetic field strengths. The circles show the prediced placement of the lines calculated using the Breit-Rabi formula. Black circles are for $F = I + 1/2$ and the grey circles are for $F = I - 1/2$. In each case, the predicted values were shifted so that the first prediction lines up with the first line, to compensate for variations in the background magnetic field.

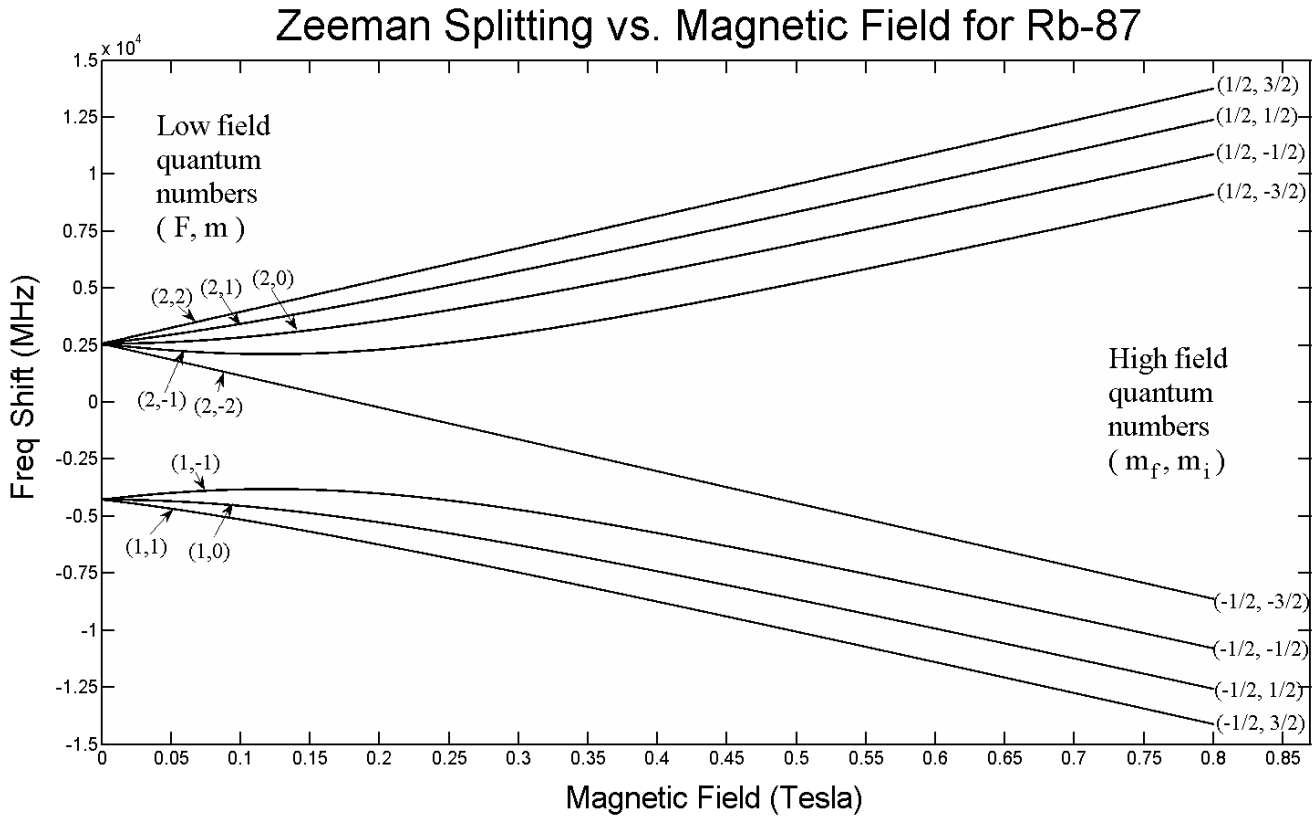

FIG. 3. Plot of the Breit-Rabi equation, showing the rearrangement of the lines at high fields. The magnetic fields we produced were all $< .001T$.

$T = 42\,^{\circ}\mathrm{C}$) is

$$\delta\nu_D = \frac{4}{\lambda_0}\left(\frac{2\ln(2)kT}{m}\right)^{1/2} = 2.73Hz \qquad (10)$$

which is clearly much smaller. Power broadening only becomes greater than lifetime broadening in the optical frequencies.

To look for power broadening, we measured the Rb-8 line with zero applied field for 7 power levels ranging from .001mW to 1mW. The power consumed by the Helmholtz coils was calculated using the equation

$$P = \frac{V^2}{Z} = \frac{V^2}{\sqrt{\omega L^2 + R^2}} \qquad (11)$$

where the impedance of the Helmholtz pair was estimated to be approximately .5Ω and R was measured to be 1.5Ω.

These lineshapes were fit to a (weighted) linear sum of a Gaussian and a Lorentzian. The FWHM of both were calculated to see if any evidence of broadening could be determined, the results of which are shown in Figure 4. The values for χ^2/DOF for these fits varied between .8 and .2, corresponding to $p <$ and $p <$. As expected, the FWHM of the Gaussian is smaller, but there is no evidance of power broadening. (Note, the magnitude of these FWHM numbers should not be taken too literally,

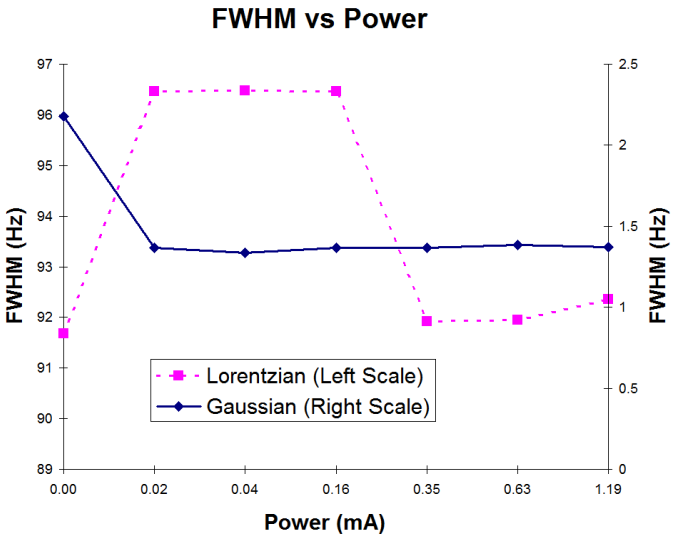

FIG. 4. Search for power broadening.

as there were also scale factors ("weights") which were not included)

As we calculated before, the Doppler broadening thus is very small. However, we found that our lineshapes

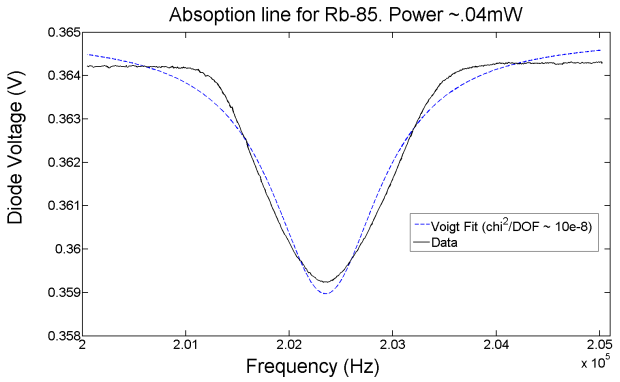

FIG. 5.

are better characterized by a Gaussian lineshape alone than a Lorentzian. This suggests there is another form of inhomogeneous broadening present, ie. broadening which, like Doppler broadening, results in otherwise identical atoms having different resonance frequencies (For instance, small fluctuations / spatial variations in the magnetic field).

Taking into account both pressure broadening and Doppler/inhomogenous broadening involves doing a convolution of both the Guassian and Lorentzian lineshapes. The result is the "Voigt Profile" which (after extensive manipulations) can be expressed in terms of the complex error function and the afforementioned FWHM's as

$$\begin{aligned} S(\nu) &= \frac{.939}{\delta\nu_D}\Re\{\mathrm{erfc}(x+ib)\} \\ x &\equiv 3.34\frac{\nu_0-\nu}{\delta\nu_D} \\ b &\equiv 3.34\frac{\delta\nu_0}{\delta\nu_D} \end{aligned} \tag{12}$$

A MATLAB program was used to try to fit the lineshape to the Voigt profile. Then, the FWHM of the Voigt profile can be calculated within two percent in terms of the FWHM's (f's) of the Lorentz and Gaussian components as: (Olivero, pg 233)

$$f_\mathrm{V} \approx 0.5346 f_\mathrm{L} + \sqrt{0.2166 f_\mathrm{L}^2 + f_\mathrm{G}^2} \tag{13}$$

or by numerical means. An example fit is shown in Figure 5.

ACKNOWLEDGMENTS

Thanks to Prof. Weinacht for his help and advice.

Appendix A: Hyperfine structure & Zeeman splitting

The first contribution to the splitting of a given energy level is the fine structure which is due to coupling of the electron's spin with the magnetic field it sees from its motion around the proton. The good quantum number becomes $J = L + S$.

The hyperfine structure is due to coupling of the electron's spin with the magnetic moment of the nucleus. The primary correction comes from the dipole moment of the nucleus, which is due to both the intrinsic spin angular momentum of the protons and neutrons and their orbital angular momentum within the nucleus. In CGS units it is defined as:

$$\vec{\mu}_N \equiv -g_I \frac{e}{2m_p c}\vec{I} \tag{A1}$$

Here I is the total spin of the nucleus and g_I is the nuclear g-factor, which is very difficult to calculate, but can be found experimentally. The shift in energy is $\Delta E = -\vec{mu}\cdot \vec{H}(0)$, where $\vec{H}(0)$ is the magnetic field at the nucleous. The direction of $\vec{H}(0)$ is the same as the total angular momentum of the electrons, so

$$\Delta E = \left(\frac{\mu_N H(0)}{|I||J|}\right)\vec{I}\cdot\vec{J} \tag{A2}$$

The total angular momentum is $\vec{F} = \vec{J} + \vec{I}$, and the good quantum number becomes $F = J + I$, which can take integer or half-integer values $|J - I| \le F \le |J + I|$. The Zeeman splitting is a splitting of these otherwise degenerate m_F levels. The Hamiltonian which includes both the hyperfine and Zeeman interactions is

$$H = hA\vec{I}\cdot\vec{J} - \mu_B(g_J\vec{J} +_I \vec{I})\cdot\vec{B} \tag{A3}$$

For $J = 1/2$ this Hamiltonian can be solved exactly, resulting in the Breit-Rabi equation:

$$\begin{aligned} \Delta E_{F=I\pm1/2} &= \frac{-hA}{2(2I+1)} + \mu g_I m_F B \pm \frac{hA}{2}\sqrt{1+\frac{2m_F x}{I+1/2}+x^2} \\ x &\equiv \frac{\mu_B B(g_J - g_I)}{hA} \end{aligned} \tag{A4}$$

where x is referred to as the "field strength parameter". (Note: for $> m = -(I + 1/2)$ the square root is an exact square, and should be interpreted as $+(1 - x)$). Notably, the electric quadrapole interaction is zero for $L = 0, J = 1/2$, so this formula is fairly accurate.

Appendix B: Derivation of the Breit-Rabi formula

(note: this portion was posted on Wikipedia under the article "Zeeman effect" by the primary author). In the magnetic dipole approximation, the Hamiltonian which includes both the hyperfine and Zeeman interactions is

$$\begin{aligned} H &= hA\vec{I}\cdot\vec{J} - \mu\cdot\vec{B} \\ H &= hA\vec{I}\cdot\vec{J} - \mu_B(g_J\vec{J} + g_I\vec{I})\cdot\vec{B} \end{aligned} \tag{B1}$$

To arrive at the Breit-Rabi formula we will include the hyperfine structure (interaction between the electron's spin and the magnetic moment of the nucleus), which is governed by the quantum number $F \equiv |\vec{F}| = |\vec{J} + \vec{I}|$, where $\vec{I}$ is the spin angular momentum operator of the nucleus. Alternatively, the derivation could be done with J only. The constant A is known as the zero field hyperfine constant and is given in units of Hertz. μ_B is the Bohr magneton. $\hbar\vec{J}$ and $\hbar\vec{I}$ are the electron and nuclear angular momentum operators. g_J and g_F can be found via a classical vector coupling model or a more detailed quantum mechanical calculation to be:

$$\begin{aligned} g_J =& g_L \frac{J(J+1) + L(L+1) - S(S+1)}{2J(J+1)} \\ &+ g_S \frac{J(J+1) - L(L+1) + S(S+1)}{2J(J+1)} \\ g_F =& g_J \frac{F(F+1) + J(J+1) - I(I+1)}{2F(F+1)} \\ &+ g_I \frac{F(F+1) - J(J+1) + I(I+1)}{2F(F+1)} \end{aligned}$$

As discussed, in the case of weak magnetic fields, the Zeeman interaction can be treated as a perturbation to the $|F, m_f\rangle$ basis. In the high field regime, the magnetic field becomes so large that the Zeeman effect will dominate, and we must use a more complete basis of $|I, J, m_I, m_J\rangle$ or just $|m_I, m_J\rangle$ since I and J will be constant within a given level.

To get the complete picture, including intermediate field strengths, we must consider eigenstates which are superpositions of the $|F, m_F\rangle$ and $|m_I, m_J\rangle$ basis states. For $J = 1/2$, the Hamiltonian can be solved analytically, resulting in the Breit-Rabi formula. Notably, the electric quadrapole interaction is zero for $L = 0$ ($J = 1/2$), so this formula is fairly accurate.

To solve this system, we note that at all times, the total angular momentum projection $m_F = m_J + m_I$ will be conserved. Furthermore, since $J = 1/2$ between states m_J will change between only $\pm 1/2$. Therefore, we can define a good basis as:

$$|\pm\rangle \equiv |m_J = \pm 1/2, m_I = m_F \mp 1/2\rangle \qquad \text{(B2)}$$

We now utilize quantum mechanical ladder operators, which are defined for a general angular momentum operator L as

$$L_\pm \equiv L_x \pm i L_y \qquad \text{(B2)}$$

These ladder operators have the property

$$L_\pm |L, m_L\rangle = \sqrt{(L \mp m_L)(L \pm m_L + 1)}\,|L, m_L \pm 1\rangle \quad \text{(B2)}$$

as long as m_L lies in the range $-L, \ldots ..., L$ (otherwise, they return zero). Using ladder operators $J_\pm$ and $I_\pm$ We can rewrite the Hamiltonian as

$$H = hAI_z J_z + \frac{hA}{2}(J_+ I_- + J_- I_+) - \mu_B B(g_J J_z + g_I I_Z) \qquad \text{(B2)}$$

Now we can determine the matrix elements of the Hamiltonian:

$$\langle \pm|H|\pm\rangle = -\frac{1}{4}A - \mu_B B g_I m_F \pm \frac{1}{2}(hA m_F - \mu_B B(g_J - g_I)) \qquad \text{(B2)}$$

$$\langle \pm|H|\mp\rangle = \frac{1}{2}hA\sqrt{(I + 1/2)^2 - m_F^2} \qquad \text{(B2)}$$

Solving for the eigenvalues of this matrix, (as can be done by hand, or more easily, with a computer algebra system) we arrive at the energy shifts for $F = I \pm 1/2$:

$$\Delta E = \frac{-h\Delta W}{2(2I+1)} + \mu_B g_I m_F B \pm \frac{h\Delta W}{2}\sqrt{1 + \frac{2m_F x}{I + 1/2} + x^2} \qquad \text{(B2)}$$

$$x \equiv \frac{\mu_B B(g_J - g_I)}{h\Delta W} \qquad \Delta W = A\left(I + \frac{1}{2}\right) \qquad \text{(B2)}$$

where ΔW is the splitting (in units of Hz) between two hyperfine sublevels in the absence of magnetic field B, and x is referred to as the 'field strength parameter' (Note: for $m = -(I + 1/2)$ the square root is an exact square, and should be interpreted as $+(1 - x)$). This equation is known as the Breit-Rabi formula and is useful for systems with one valence electron in an s ($J = 1/2$) level (Woodgate, 1993).

REFERENCES

[1] G. Breit and I. Rabi, Phys. rev. 38, 2082 (1931)

[2] MW Milonni and JH Eberly. *Lasers* First Edition. John Wiley & Sons 1988.

[3] Olivero, J.J.; R.L. Longbothum (1977-02). "Empirical fits to the Voigt line width: A brief review". Journal of Quantitative Spectroscopy and Radiative Transfer 17 (2): 233236.

[4] GK Woodgate, *Elementary Atomic Structure*, Oxford University Press 1983. Section 9.